Optimizing Cylindrical Antennas for Cost Savings Using Non-Integer Arrays

Roopesh Kumar Polaganga
Department of Electrical Engineering
University of Texas at Arlington
Arlington, TX 76019-0016, USA
email: roopeshkumar.polaganga@mavs.uta.edu

Qilian Liang
Department of Electrical Engineering
University of Texas at Arlington
Arlington, TX 76019-0016, USA
email: liang@uta.edu

***Abstract*— This study introduces a cost-effective and spectrally efficient approach to deploying cylindrical antenna arrays in cellular networks using non-integer array configurations. Traditional integer-based arrays require many antenna elements, increasing infrastructure costs and deployment complexity. By adopting non-integer spacing both vertically and horizontally, our method shows that fewer elements are needed while maintaining or enhancing beam strength and focus. Simulations confirm that non-integer arrays improve beam characteristics, sum-rate capacity, and spectral efficiency, thanks to reduced mutual coupling and lower signal correlation, especially in multipath channels. This approach offers a viable, cost-effective alternative for next-generation wireless technologies, including 6G networks.**

***Index Terms*— Cylindrical Antenna Arrays, Non-Integer Arrays, Rational Arrays, Cellular Networks, 6G.**

I. INTRODUCTION

Antenna arrays are crucial for modern wireless communication, particularly cylindrical arrays known for high gain and directivity in cellular base stations. Traditionally, these arrays use integer-spaced configurations, placing sensors at integer multiples of half the wavelength (λ), valued for their simplicity and ease of implementation across various applications like radar and sonar [1]. However, this rigidity results in high material and deployment costs due to the large number of required elements.

Recent advancements propose non-integer spacing, placing antenna elements at non-integer multiples of the wavelength, reducing the number of elements while maintaining or enhancing performance metrics such as array factor and beamwidth [2]. Sparse and coprime arrays, using the difference co-array concept to identify more sources than physical elements, have shown potential but are limited by integer spacing [3]. Similarly, unequally spaced arrays typically adhere to integer spacings, limiting flexibility in dynamic cellular networks [4]. Strategies like femtocells [5], joint processing across cell sites [6], and distributed antenna systems [7] enhance capacity but also increase costs. Non-integer arrays offer a transformative shift, allowing sensor placements at rational multiples of the wavelength (λ), providing exceptional design flexibility [8]. This is particularly relevant for next-generation technologies like 6G, which demand innovative antenna designs for higher frequency bands and precise beamforming [9]. Non-integer spaced arrays reduce physical resource needs while enhancing adaptability and scalability, aligning with the future needs of wireless networks for cost-effective and versatile antenna configurations.

This work was supported in part by the U.S. National Science Foundation under Grant CCF-2219753.

A. Related work

In a series of publications, Kulkarni P. et al. [19-20] explored rational non-integer sensor locations in linear arrays, significantly improving Direction of Arrival (DOA) estimation and source resolution even in low SNR and with limited snapshots. They also touched on theoretical concepts of irrational sensor locations to enhance array performance [2]. Additionally, non-uniform antenna arrays and multi-frequency techniques for improved DOA estimation were explored, addressing mutual coupling practically [10]. Optimal non-redundant arrays (ONRAs) were designed using non-integer multiples, improving DOA estimation accuracy and reducing mutual coupling [11]. Square Heffter arrays in graph theory were extended to non-integer arrays [12], and non-integer arrays demonstrated enhanced spectral efficiency and capacity in cellular networks beyond DOA estimations but limited to Uniform Linear Arrays (ULAs) [13]. Extension to cylindrical arrays is considered in [14].

Cylindrical antenna arrays have been studied for radar applications, enhancing direction-of-arrival estimation and system performance. Eight-element arrays for MIMO radar applications showed stable azimuthal plane performance. Cylindrical arrays tailored for DOA estimation maintained uniform performance across viewing angles [15]. Sparse cylindrical arrays enhanced Massive MIMO systems' performance by incorporating sparse, co-prime, and nested structures, reducing physical antennas while improving spatial resolution and channel capacity, but were limited to integer arrays [16]. This work addresses the unexplored deployment of non-integer spaced cylindrical antenna arrays in cellular networks, optimizing network performance and reducing antenna elements. Our simulations demonstrate that non-integer arrays maintain beam pattern integrity, significantly reduce the number of antenna elements, and enhance capacity and spectral efficiency compared to traditional integer-based arrays.

2024 IEEE Virtual Conference on Communications (VCC) | 979-8-3315-3009-9/24/$31.00 ©2024 IEEE | DOI: 10.1109/VCC63113.2024.10914356

B. Scope and outline

Unlike previous applications focused on target estimation, this paper explores non-integer array-based transmitter antennas at base stations in cellular networks. We analyze and simulate two-dimensional cylindrical array antennas, highlighting their beam pattern characteristics. Optimization of antenna element locations for optimal performance is planned for future research.

This paper is organized as follows - section-II Introduces the number theory of non-integer arrays in cellular networks, presenting two key axioms crucial for understanding the subsequent formulations. Section-III discusses the two-dimensional cylindrical array antenna and formulates the array factor and sum-rate capacity for non-integer-based arrays, demonstrating improved performance over traditional integer-based arrays. Section-IV covers the MATLAB simulation results to demonstrate the gains. Section-V concludes the results along with additional details on future work.

II. Cylindrical Antenna Design with Non-Integer Arrays

A. Cylindrical Antenna Array

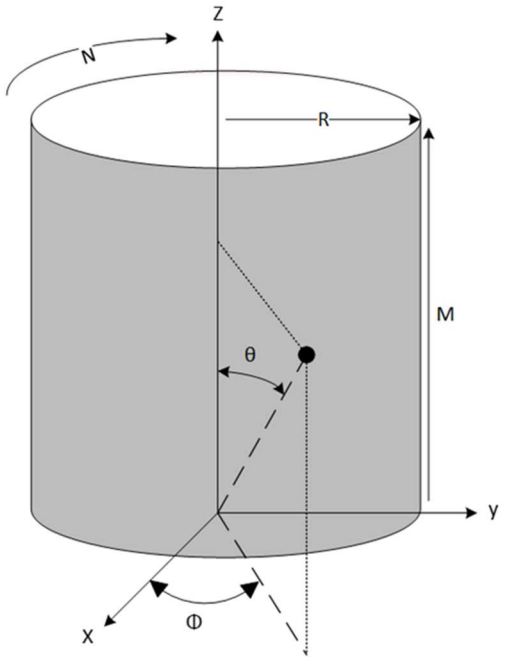

Fig. 1. Cylindrical Antenna Array

The cylindrical array in this study consists of multiple circular arrays stacked vertically. Each circular array has uniformly spaced elements positioned along the circumference, enabling beamforming in both azimuth and elevation planes. This design provides high directivity and low side lobe levels, ideal for radar and telecommunications applications. The array has M stacked circular arrays, each with N element and radius R. Element in the circular array is positioned at angular intervals to ensure uniform spacing. The angular position of the n^{th} element is $\emptyset_n = 2\pi n/N$ where $n = 0,1,2\ldots N-1$. The cartesian coordinates are $x_n = R\cos(\emptyset_n)$ and $y_n = R\sin(\emptyset_n)$. The height z_m of the m^{th} circular array is $z_m = m \cdot dz$ where dz is the vertical spacing.

The phase shift for each element is calculated based on its horizontal and vertical positions. The horizontal phase shift due to azimuth angle $\emptyset$ and the position angle $\emptyset_n$ is $\Delta\emptyset_{horizontal} = \kappa \cdot R \cdot \sin(\theta) \cdot \cos(\emptyset - \emptyset_n)$ where $\kappa = \frac{2\pi}{\lambda}$ is the wavenumber, R is the radius, θ is the elevation angle, $\emptyset$ is the fixed azimuth angle and $\emptyset_n$ is the position angle. The vertical phase shift due to elevation angle θ and the vertical position z_m is $\Delta\emptyset_{vertical} = \kappa \cdot z_m \cdot \cos(\theta)$. The total phase shift for an element at position (n, m) is,

$$\Delta\emptyset_{Total} = \kappa \cdot R \cdot \sin(\theta) \cdot \cos(\emptyset - \emptyset_n) + \kappa \cdot z_m \cdot \cos(\theta) \quad (1)$$

The array factor (AF) sum of the contributions of each element's positioned at (x_n, y_n, z_m):

$$AF(\theta, \emptyset) = \sum_{m=0}^{N_c-1} \sum_{n=0}^{N-1} A(n,m) \cdot e^{j\Delta\emptyset_{Total}} \quad (2)$$

where $A(n,m)$ is the amplitude excitation of the element at position (n,m). This work extends the derivation from integer-based to non-integer-based arrays while maintaining consistent array size, addressing physical constraints in real-world applications.

B. Optimization along Z-Plane & XY-Plane

Comparing the beam patterns for both integer and non-integer cylindrical arrays emphasized on vertical axis results to the reduction of the circular array count while maintaining the same overall height of the cylinder. Integer array with $N_{c\mathbb{I}}$ circular arrays and vertical spacing of $dz_{\mathbb{I}}$ resulting in the height of $(N_{c\mathbb{I}} - 1) \times dz$. Vertical positions of circular arrays are $z_{m\mathbb{I}} = m \cdot dz_{\mathbb{I}}$ where $m = 0,1,2..N_{c\mathbb{I}} - 1$. For non-integer cylindrical array, the number of circular arrays $N_{c\mathbb{N}}$ and adjusted vertical spacing $dz_{\mathbb{N}}$ ensure similar height as the integer array:

$$dz_{\mathbb{N}} = \frac{(N_{c\mathbb{I}}-1)\times dz_{\mathbb{I}}}{N_{c\mathbb{N}}-1} \quad (3)$$

This allows reducing $N_{c\mathbb{N}}$ while maintaining the form-factor shown as $dz_{\mathbb{I}} \geq dz_{\mathbb{N}}\ \forall\ N_{c\mathbb{N}} \leq N_{c\mathbb{I}}$. The coprimality concept ensures vertical spacings do not share common factors, minimizing mutual interference and optimizing beamforming. For simplicity, this study considers equal spacing in simulations, but the derivations apply to unequal spacing. The integer cylindrical array factor $AF_{\mathbb{I}}$ is

$$AF_{\mathbb{I}}(\theta, \emptyset) = \sum_{m=0}^{N_{c\mathbb{I}}-1} \sum_{n=0}^{N-1} A(n,m) \cdot e^{j\Delta\emptyset_{\mathbb{I}}} \quad (4)$$

With total phase shift $\Delta\emptyset_{\mathbb{I}} = \kappa \cdot \mathrm{R} \cdot \sin(\theta) \cdot \cos(\emptyset - \emptyset_n) + \kappa \cdot z_{m,\mathbb{I}} \cdot \cos(\theta)$ derived. For non-integer spacing, array factor is:

$$AF - V_{\mathbb{N}}(\theta, \emptyset) = \sum_{m=0}^{N_{c\mathbb{N}}-1} \sum_{n=0}^{N-1} A(n,m) \cdot e^{j\Delta\emptyset_{\mathbb{N}}} \quad (5)$$

With vertical position $z_{m,\mathbb{N}} = m \cdot dz_{\mathbb{N}j}$ and phase shift:

$$\Delta\emptyset_{\mathbb{N}} = \sum_{j=1}^{k} (\Delta\emptyset_{horizontal} + \kappa \cdot z_{m \cdot j} \cdot \cos(\theta)) \quad (6)$$

This approach maintains the antenna array size while improving performance through non-integer spacing on vertical plane. On the horizontal plane, the same physical size with radius R. For integer scenario, elements are positioned at equal angular intervals by $\emptyset_n = 2\pi n/N$ where N is the total number of elements and n ranging from 0 to $N-1$. In non-integer arrays, to reduce the number of elements to $M < N$, a rational coprime pair (N, M) is introduced, giving angular positions:

$$\emptyset_{n\mathbb{N}} = \frac{2\pi n_{\mathbb{N}} r}{N} \quad (7)$$

with $n_{\mathbb{N}}$ ranging from 0 to $M-1$. Cartesian coordinates of these M elements are $(R\cos\emptyset_{n\mathbb{N}}, R\sin\emptyset_{n\mathbb{N}})$. The modified horizontal phase shift is $\Delta\emptyset_{n\mathbb{N}} = \kappa \cdot \mathrm{R} \cdot \sin(\theta) \cdot \cos(\emptyset - \emptyset_{n\mathbb{N}})$. For un-equal non-integer spacing, coprime pairs A and B with $gcd(A,B) = 1$ are used, creating a larger virtual array from fewer elements. This configuration minimizes grating lobes and enhances beam focus:

$$AF - H_{\mathbb{N}}(\theta, \emptyset) = \sum_{a=0}^{A-1} \sum_{b=0}^{B-1} A(a,b) \cdot e^{j\Delta\emptyset_{n\mathbb{N}}} \quad (8)$$

where $(A,B) < M \;\forall\; \sum(A,B) = M$ and $gcd(A,B) = 1$. This improved spacing effectively uses elements to focus the beam and reduce grating lobes.

C. Mutual Coupling

When designing cylindrical antenna arrays, mutual coupling must be considered, especially when reducing the number of antenna elements. Mutual coupling refers to the electromagnetic interaction between nearby antenna elements, which can induce currents in neighboring elements, affecting impedance and the overall radiation pattern [7]. In cylindrical arrays, mutual coupling impacts performance due to varied spatial relationships between elements. It can be represented using a impedance matrix $\mathbf{Z}$ of size $N \cdot M \times N \cdot M$. Each element $\mathbf{Z}_{ij}$ represents the mutual impedance between elements i and j with coordinates (x_i, y_i, z_i) and (x_j, y_j, z_j). The distance between elements is

$$d_{ij} = \sqrt{R_A + R_B + (z_i - z_j)^2} \quad (9)$$

where $R_A = \left(r_i \cos(\emptyset_i) - r_j \cos(\emptyset_j)\right)^2$ and $R_B = \left(r_i \sin(\emptyset_i) - r_j \sin(\emptyset_j)\right)^2$ while the total impedance is expressed as $\mathbf{Z}_{ij} = \boldsymbol{R}_{ij} + j\boldsymbol{X}_{ij}$ with both $\boldsymbol{R}_{ij}$ (mutual resistance) and $\boldsymbol{X}_{ij}$ (mutual reactance) being function of d_{ij}. Uniformly spaced elements in integer arrays result in consistent mutual coupling but higher signal correlation, limiting spatial diversity. Non-integer spaced arrays reduce mutual coupling and signal correlation due to irregular element positioning, enhancing spatial diversity and improving sum-rate capacity and spectral efficiency, despite potential grating lobes in the beam pattern.

D. System Design

When designing cellular networks with non-integer cylindrical arrays, we model the transmitted and received signals at the base station to leverage spatial diversity and signal discrimination, particularly in multi-user scenarios under Rayleigh fading conditions. The received signal y at the base station from K users is modeled as $y = \boldsymbol{H}X + n$. Here, y is the $N \times M$ received signal vector, $\boldsymbol{H}$ is the $N \times K$ channel matrix with elements undergoing independent Rayleigh fading, x is the $K \times 1$ transmitted signal vector, and n is the $N \times M$ complex gaussian noise vector $\mathcal{CN}(0, \sigma^2 \boldsymbol{I}_{N\times M})$. For the downlink sum-rate capacity in a multi-user (MU-MIMO) setting, we consider a base station with $N \times M$ element cylindrical antenna array. The downlink sum-rate capacity $C_{\mathbb{I}}$ for an integer array, assuming linear precoding and prefect CSI, is

$$C = \log_2 \det\left(\mathrm{I}_K + \frac{\rho}{K\sigma^2} \boldsymbol{H}\boldsymbol{H}^H\right) \quad (10)$$

For integer arrays, elements are spaced by integer multiples of half the wavelength ($\lambda/2$). The channel matrix $\boldsymbol{H}$ reflects the pathloss, phase shift, and multipath fading. The element h_{ijk} of $\boldsymbol{H}$ incorporates the phase difference due to path length difference as $h_{ijk} = \alpha_{ijk} e^{-j(i-1)\Delta\emptyset_i \cdot -j(j-1)\Delta\emptyset_j}$ where $\Delta\emptyset_i, \Delta\emptyset_j = \frac{2\pi}{\lambda} d\,(\sin(\theta), \cos(\theta))$. Non-integer arrays, with $\boldsymbol{H}_{\mathbb{N}}$, offer better spatial diversity than integer arrays ($\boldsymbol{H}_{\mathbb{I}}$) by reducing mutual coupling and signal correlation. The determinant of the correlation matrix $R = \mathbb{E}[\boldsymbol{H}\boldsymbol{H}^{\boldsymbol{H}}]$ is higher for non-integer arrays, enhancing sum-rate capacity. Thus, for integer array, $det(\boldsymbol{H}_{\mathbb{I}}\boldsymbol{H}_{\mathbb{I}}^{\boldsymbol{H}}) = \boldsymbol{det}(R_{\mathbb{I}}) \leq \sigma^{2N}$ and for non-integer arrays, $det(\boldsymbol{H}_{\mathbb{N}}\boldsymbol{H}_{\mathbb{N}}^{\boldsymbol{H}})$ is not bound by Hadamard's product of diagonals due to non-zero diagonal elements. Since the determinant is a product of eigenvalues, a broader spread (assuming the mean of the eigenvalues is the same) means $\det(R_{\mathbb{N}}) \geq \det(R_{\mathbb{I}})$.

Spectral efficiency $\gamma = C/B = \log_2(1+\rho)$, where $\rho = \mathrm{P}/\sigma^2$, has upper ($S_{UB}$) and lower ($S_{LB}$) bounds related to the eigen values of the normalized channel matrices. The slopes of the bounds are:

$$S_{UB,\mathbb{I}} = \frac{d\gamma_{UB,\mathbb{I}}}{dlog(\rho)};\quad S_{UB,\mathbb{N}} = \frac{d\gamma_{UB,\mathbb{N}}}{dlog(\rho)} \qquad (11)$$

$$S_{LB,\mathbb{I}} = \frac{d\gamma_{LB,\mathbb{I}}}{dlog(\rho)};\quad S_{LB,\mathbb{N}} = \frac{d\gamma_{LB,\mathbb{N}}}{dlog(\rho)} \qquad (12)$$

Non-integer arrays, with enhanced spatial diversity, are expected to perform closer to the upper bound, offering improved sum-rate capacity and spectral efficiency compared to integer arrays [21, 22].

III. Results

To demonstrate the technical feasibility of the derivation, MATLAB simulations were conducted in multiple setups. The existing integer array framework in [17] was updated to accommodate non-integer arrays using the approach outlined earlier. The carrier frequency was set to 2.5 GHz with a 100 MHz bandwidth, reflecting the Sub-6GHz band (n41) used in 5G TDD as specified by 3GPP. A 32-transmit M-MIMO configuration was used, common for this band. For base cylindrical array simulation, 10 circular arrays ($N_{c,\mathbb{I}} = 10$) were spaced vertically at $dz_{\mathbb{I}} = 0.5$m, forming a total height of $(N_{c\mathbb{I}} - 1) \times dz_{\mathbb{I}} = 9 \times 0.5 = 4.5meters$. The vertical positions of circular arrays are $z_{m,\mathbb{I}} = m \cdot dz_{\mathbb{I}}$ where $m = 0,1,2..N_{c\mathbb{I}} - 1$ are [0,0.5,1,..4.5] meters. Each circular array has 32 antenna elements, totaling $32 \times 10 = 320$ elements as shown in Fig.2 in reference to [18]. For all simulations, the array factor was normalized to its maximum value and converted to dB. The elevation angle in degrees was plotted against the normalized beam pattern in dB, focusing on the main lobe and nearby side lobes around 90 degrees. Simulations were performed using MATLAB-2024a, calculating the beam pattern for elevation angles θ from 0 to π radians (0 to 180 degrees). The azimuth angle $\emptyset$ is fixed at 0 degrees.

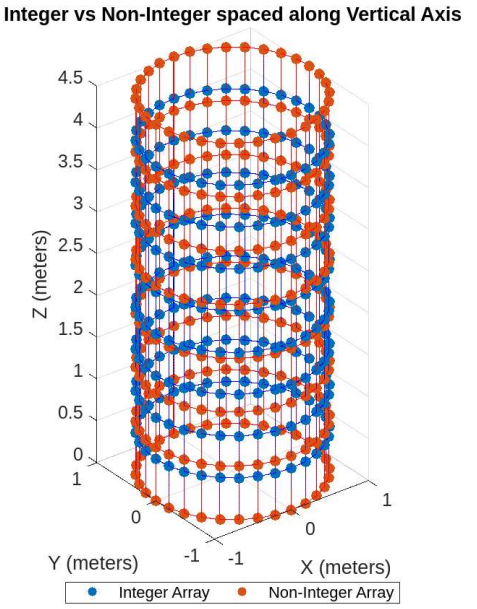

Fig. 2. Vertical Axis Spacing: integer vs. non-integer

Fig.2 provides a three-dimensional visualization of cylindrical antenna arrays, contrasting integer-spaced and non-integer spaced configurations along the vertical axis. The blue elements represent the integer-spaced array, where $N_{c\mathbb{I}}$ circular arrays are uniformly distributed, ensuring consistent vertical spacing of $dz_{\mathbb{I}}$. In contrast, the red elements illustrate the non-integer spaced array with total count of $N_{c\mathbb{N}} = 8$, where elements are strategically positioned using non-integer multiples of the wavelength i.e., $dz_{\mathbb{N}}$, allowing for fewer circular arrays while maintaining the same height of $(N_{c\mathbb{I}} - 1) \times dz = 4.5m$. Such spacing approach demonstrates how non-integer configurations can effectively reduce the number of circular arrays required by $N_{c\mathbb{I}} - N_{c\mathbb{N}} = 2$ without compromising the structural integrity or performance of the array.

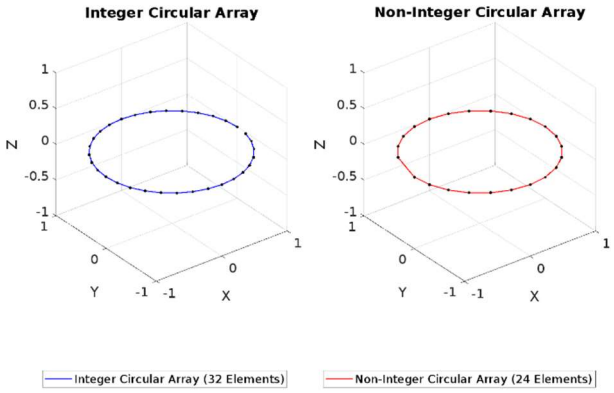

Fig. 3. Horizontal Axis Spacing: integer vs. non-integer

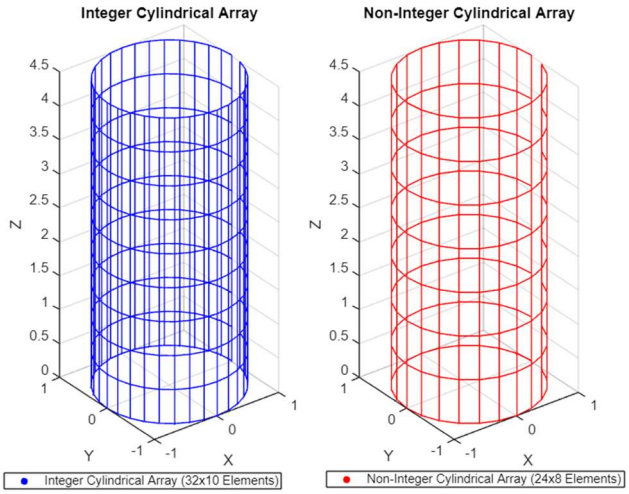

Fig. 4. Horizontal and Vertical Spacing: Integer vs. Non-Integer

On the horizontal axis, in comparison to the initial integer based cylindrical array has 32 antenna elements per single circular array and a single circular array is shown on the left side of Fig.3 with each antenna element shown as a block-dot and all 32 elements are connected to form circular array. To minimize the antenna elements to 24, coprime pairs like (19,5)

or (17,7) and (13,11) are considered whose gcd is one and sums to 24 with an overall reduction of 8 antenna elements per circular array. Out of all the available pairs, (13,11) is the has the closest value, leading to a more uniform distribution of elements which can help in maintaining the main lobe strength and providing a more consistent beam pattern with less severe grating lobes.

Fig. 4 compares 3D visualizations of cylindrical antenna arrays with integer and non-integer spacing. The left subfigure shows the integer configuration (blue), featuring 320 elements: 32 elements per circular array across 10 vertical stacks. The right subfigure presents the non-integer configuration with 192 elements: 24 elements per array across 8 vertical stacks, reducing elements by approximately 40%. This non-integer approach optimizes element placement using coprime pairs, maintaining the array's physical dimensions while highlighting cost-effective deployment with fewer elements.

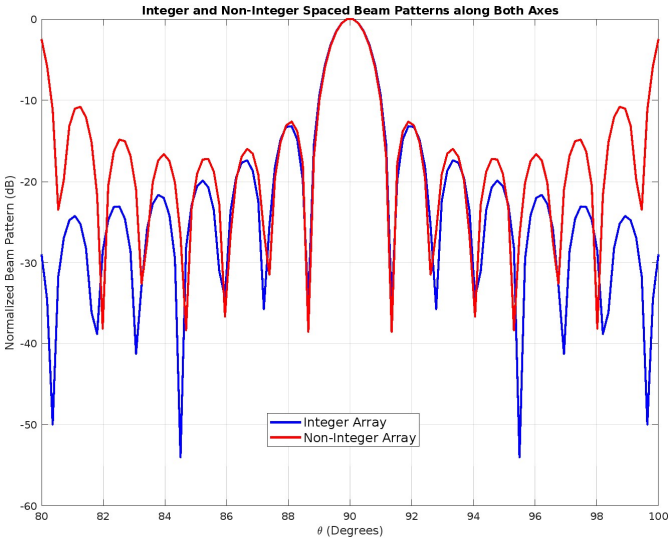

Fig. 5. Beam Pattern Analysis: Integer vs. Non-Integer Spacing on Both Axes

Fig.5 depicts the beam pattern comparison between the integer and non-integer spaced cylindrical antenna arrays. The integer array beam pattern, shown in blue, serves as the baseline for evaluating the performance improvements achieved by the non-integer array, displayed in red. Both configurations have the main lobe centered at 90 degrees, with the non-integer array demonstrating slightly higher main lobe intensity. However, the non-integer array exhibits increased grating side lobes, indicating a trade-off between main lobe enhancement and side lobe suppression. This comparison highlights the efficacy of non-integer spacing in enhancing beam strength while maintaining the overall beam pattern structure, despite the observed increase in sidelobes. The results suggest that non-integer spacing can effectively reduce the number of required antenna elements, providing a more cost-efficient solution without substantially compromising the array's performance.

Fig.6 presents a comparison of sum-rate capacity as a function of SINR for integer and non-integer antenna array configurations, as computed by Eq. (18). The graph delineates the performance of integer (blue curve) versus non-integer (red dashed curve) array spacings. Notably, the non-integer array consistently outperforms the integer array across the SINR spectrum, with the disparity in capacity becoming increasingly significant at higher SINR levels. Quantitatively, the non-integer array shows an average improvement of approximately 60.8% over the integer array. This performance enhancement translates to an average increase of 3867.8 bits/s/Hz in sum-rate capacity, underscoring the efficiency of non-integer spacing in high SINR regimes, which is critical for optimizing system throughput in advanced wireless communication systems.

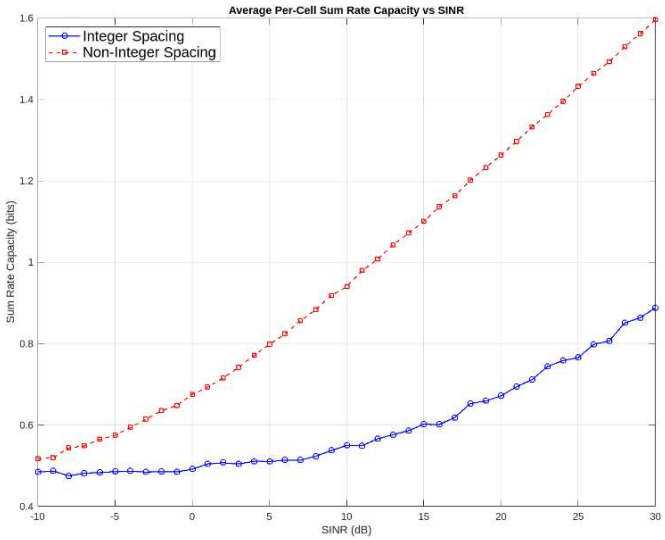

Fig. 6. Integer vs. Non-Integer Spaced Cylindrical Arrays: Sum-Rate Capacity and SINR

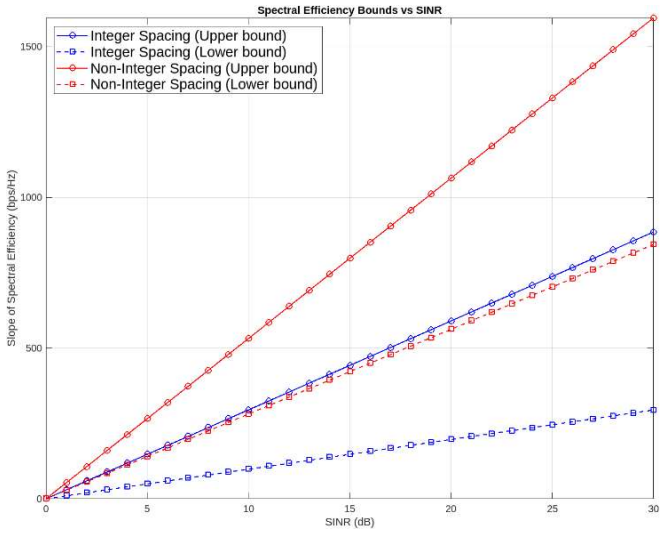

Fig. 7. Integer vs. Non-Integer Spaced Cylindrical Arrays: Spectral Efficiency and SINR

Fig. 7 illustrates the bounds on spectral efficiency as a function of SINR for cylindrical antenna arrays utilizing integer and non-integer element spacing. The graph delineates the upper and lower bounds of the spectral efficiency slope, represented by solid and dashed lines, respectively. For the integer spacing scenario, the bounds are indicated by blue lines, while the red lines represent the non-integer spacing scenario. The non-integer array configurations consistently demonstrate superior bounds compared to their integer counterparts, corroborating the theoretical enhancement postulated. The average increase in the maximum spectral efficiency slope is quantified at 21.3 bps/Hz, while the minimum slope sees an average rise of 18.2 bps/Hz. This data graphically validates the theoretical assertion that non-integer spacing can lead to substantial improvements in the spectral efficiency of antenna arrays, which is critical for bandwidth optimization in wireless communication systems.

IV. Conclusion and Future Work

This study presents a comprehensive analysis of cylindrical antenna arrays with non-integer spacing configurations, focusing on cost reduction and performance optimization in cellular networks. By adopting non-integer spacing both vertically and horizontally, we demonstrated the potential to maintain or enhance beam strength and focus while significantly reducing the number of required antenna elements by 40% (from 320 to 192). Our simulations showed that non-integer arrays maintain overall beam pattern integrity and main lobe characteristics, with a slight increase in grating sidelobe levels. The reduced mutual coupling resulting from fewer antenna elements led to a significant improvement in sum-rate capacity by over 60%, and the spectral efficiency slope bounds improved by 18 and 21 bps/Hz. These results indicate that non-integer spacing offers a promising alternative to traditional integer-based configurations, potentially reducing deployment costs and the environmental impact of antenna arrays in wireless communication systems.

Future research will extend this study by incorporating dynamic element placement algorithms that adapt to real-time network requirements and environmental conditions. Additionally, an in-depth analysis of the trade-offs between sidelobe levels and main lobe enhancements can be conducted to develop strategies for sidelobe mitigation. Further investigation will explore the application of non-integer spacing in other antenna array geometries and its impact on advanced communication technologies crucial for future 6G networks. Integrating non-integer arrays with advanced signal processing techniques, such as adaptive beamforming and machine learning-based optimization, will also be explored to enhance spectral efficiency and capacity in next-generation wireless networks.

V. References

[1] Kabacik, Pawel & Bialkowski, M.E. (2011). Cylindrical array antenna and their applications in wireless communications systems.

[2] Kulkarni, Pranav & Vaidyanathan, P. (2022). Non-Integer Arrays for Array Signal Processing. IEEE Transactions on Signal Processing. PP. 1-16. 10.1109/TSP.2022.3221862.

[3] Y. D. Zhang, M. G. Amin, and B. Himed, "Sparse Array Processing Using Coprime Arrays and Mixed Radix Coarrays," IEEE Transactions on Signal Processing, vol. 63, no. 2, pp. 331-345, Jan 2015.

[4] Jana, Rittwik & Dey, Subhrakanti. (2000). Mobile capacity enhancement using unequally spaced antenna arrays. Vehicular Technology Conference, 1988, IEEE 38th. 2. 1215 - 1219 vol.2. 10.1109/VETECS.2000.851318.

[5] Andrews, Jeffrey & Claussen, Holger & Dohler, Mischa & Rangan, Sundeep & Reed, Mark. (2012). Femtocells: Past, Present, and Future. IEEE Journal on Selected Areas in Communications. 30. 10.1109/JSAC.2012.120401.

[6] Somekh, Oren & Zaidel, Benjamin & Shamai, Shlomo. (2008). Sum Rate Characterization of Joint Multiple Cell-Site Processing. Information Theory, IEEE Transactions on. 53. 4473 - 4497. 10.1109/TIT.2007.909170.

[7] Choi, Wan & Andrews, Jeffrey. (2007). Downlink Performance and Capacity of Distributed Antenna Systems in a Multicell Environment. Wireless Communications, IEEE Transactions on. 6. 69 - 73. 10.1109/TWC.2007.05207.

[8] P. Pal and P. P. Vaidyanathan, "Nested Arrays: A Novel Approach to Array Processing with Enhanced Degrees of Freedom," IEEE Transactions on Signal Processing, vol. 58, no. 8, pp. 4167-4181, Aug. 2010.

[9] Dang, S., Amin, O., Shihada, B., & Alouini, M.-S. (2020). "What should 6G be?" Nature Electronics, 3(1), 20-29.

[10] Daher, E.B. (2018). Analysis and Design of Nonuniform Arrays for Direction Finding. arXiv: Signal Processing. https://doi.org/10.48550/arXiv.1812.03091.

[11] Hosseini, Seyed & Karimi, Mahmood. (2023). Optimal Design of Non-Redundant Sparse Arrays with Non-Integer Distance between Elements. IEEE Sensors Journal. PP. 1-1. 10.1109/JSEN.2023.3295509.

[12] Cavenagh, Nicholas & Dinitz, Jeff & Donovan, Diane & Yazıcı, Sule. (2018). The existence of square non-integer Heffter arrays.

[13] R. K. Polaganga and Q. Liang, "Non-Integer Array based Antenna Deployment for Spectral Efficient Cellular Networks," submitted to IEEE Transactions on Vehicular Technology, under review.

[14] R. Polaganga, Q. Liang, Cost-Effective and Efficient Cylindrical Antenna Deployment Using Non-Integer Arrays, Submitted to IEEE Internet of Things Journal (IEEE-IOTJ), June 2024.

[15] Wu, Na & Liang, Qilian. (2017). Sparse Nested Cylindrical Sensor Networks for Internet of Mission Critical Things. IEEE Internet of Things Journal. PP. 1-1. 10.1109/JIOT.2017.2736645.

[16] Wu, Na & Zhu, Fangqi & Liang, Qilian. (2017). Evaluating Spatial Resolution and Channel Capacity of Sparse Cylindrical Arrays for Massive MIMO. IEEE Access. PP. 1-1. 10.1109/ACCESS.2017.2763599.

[17] Ilias Konsoulas (2024). Array Signal Processing Demos (https://www.mathworks.com/matlabcentral/fileexchange/55924-array-signal-processing-demos), MATLAB Central File Exchange. Retrieved April 16, 2024.

[18] Wu, Na & Liang, Qilian. (2017). Sparse cylindrical sensor network with beamforming and DoA estimation. 1-6. 10.1109/GIOTS.2017.8016239.

[19] P. Kulkarni and P. P. Vaidyanathan, "Rational Arrays for DOA Estimation," ICASSP 2022 - 2022 IEEE International Conference on Acoustics, Speech and Signal Processing (ICASSP), Singapore, Singapore, 2022, pp. 5008-5012, doi: 10.1109/ICASSP43922.2022.9746954.

[20] P. Kulkarni and P. P. Vaidyanathan, "Rational Arrays for DOA Estimation: New Insights and Performance Evaluation," 2022 56th Asilomar Conference on Signals, Systems, and Computers, Pacific Grove, CA, USA, 2022, pp. 91-95, doi: 10.1109/IEEECONF56349.2022.10051963.